Indian J. pure appl. Math., 32(10) : 1581-1590, October 2001

A NUMERICAL STUDY OF WALL-DRIVEN FLOW OF A VISCOELASTIC FLUID IN RECTANGULAR CAVITIES

H. DEMIR AND V. S. ERTURK

Department of Mathematics, Arts and Science Faculty, Ondokuz Mayis University, 55139 *Kurupelit, Samsun, Turkey*

(*Received* 14 *July* 2000; *after revision* 22 *February* 2001; *accepted* 9 *April* 2000)

In this study, in a planar cavity geometry for some time-independent non-Newtonian fluids the stability of two-dimensional flow which is generated by different wall motions was investigated. The nonlinear equations defining the flow field were solved by Gauss-Seidel iteration method numerically by using the finite-difference technique. The velocity-pressure relationship was expressed via the vorticity-stream function relationship and special attention was paid to the computations for three different values of the aspect ratio and then the results were described. The calculations were carried out for different values of the Reynolds and Weissenberg numbers. The behaviour of the vortex flow in rectangular cavities was predicted. The results were then compared with these obtained in literature for Newtonian and non-Newtonian inelastic fluids, and non-Newtonian elastic fluids results were documented first time. The agreement between the other numerical results were reasonable.

Key Words : Viscoelastic Fluid; Criminale-Erickson-Filbey (CEF) Model; Time-Independent Flow, Stability; Finite-Difference Method

INTRODUCTION

For the past several years, numerical simulation of viscoelastic flows has been a powerful tool for understanding the fluid behaviour in a variety of process of both industrial and scientific interest. Polymeric fluids, owing to their viscoelastic character, are of particular interest in the numerical simulation community because of their wide applications in materials processing and their different behaviour from that of Newtonian fluids in ways which are often complex and striking.

Numerous studies have been made on the flow of a viscous fluid in a square cavity with its upper plate sliding at a constant speed.[1] & [2]. In this paper, the flow of upper convected Criminale-Ericson-Filbey fluid has been considered and contained in an enclosed cavity with various moving walls and different geometry aspect ratios.

The cavity driven flow problem is of theoretical importance because it is a part of the larger class of test problem for both steady and unsteady flows which are reviewed and discussed in detail by Burggraf[3]. The first numerical study of driven cavity flow within an enclosed rectangular geometry was by Kawaguti[4]. He generated numerical solutions for Reynolds number up to 64. The features of the cavity flow are now well known and reproduced by others[5]. The latter authors have sought accurate numerical solutions to this problem over a range of Reynold's numbers. In 1967, Pan and Acrivos carried out the driven cavity flow with steady state Newtonian fluid flow equations and generated numerical solutions up to Reynold's number 400 for various aspect ratios. Later work was conducted by Bozermann and Dalton[1], who used various implicit finite difference methods to give a solution for Newtonian fluids in cavities with Reynold's number up to 1000. A weaker

secondary flow was obtained where a rotating vortex occupies the entire lower half of the cavity with aspect ratio 2. According to Batchelor's report[6], the general results obtained by all of the above mentioned researchers indicate that at high Re the steady ewtonian fluid flow pattern appears as a single vortex with an inviscid core possessing uniform vorticity, with any viscous effects being confined to the outer shear layers near the boundary walls. Burggraf[3] also conducted an extensive numerical study on the cavity flow problem, and examined secondary vorticies behaviour in the lower corners of the cavity. He reported that secondary vortex pattern was viscosity dominated in contrast with the relatively non-viscous primary eddy.

The cavity flow problem, for a range of Reynold's number and aspect ratio, still interests a number of researchers, both numerically and experimentally since it is the simplest model of flow with closed streamlines, and is a relative simple model for examining and validating numerical solution techniques. There are some problems in undertaking a numerical study of the fluid flows, particularly the instability which depends on grid size, (e.g. up winding) so that when Reynolds' number is increased the grid size has to be decreased. By considering such a problem some researchers have improved both the accuracy and acceleration to convergence of the Newtonian flow equations within the cavity's geometry by using various finite difference techniques such as implicit modelling, and also improving the vortivity boundary conditions. As mentioned, we have wealth Literature for cavity flow of a Newtonian fluid except non-Newtonian models. There are several reasons for this.

Joseph *et al.*[7] have demonstrated that viscoelastic effects can introduce hyperbolicity to the equation of motion at high elasticity. Brown *et al.*[8] have shown that this change of type is responsible for the deterioration of the finite-element method which is usually equipped to handle hyperbolic equations. We also wish to point out that there is no complete mathematical theory on the existence and uniqueness of viscoelastic flows. However, spectral method is known to be convergent even for hyperbolic equations[10]. Beris, Armstrong, and Brown[9] have recently developed a hybrid spectral/finite element and difference technique which are capable of very high accuracy in flow problems endowed with smooth solutions. As a result of this, Beris and co-workers have shown that convergence at Deborah numbers that are 30 times over the traditional finite-element method for the eccentric cylinder problem with an upper convected Maxwell fluid.

Also, we are aware of the work of Limpcomb *et al.*[11] who have questioned the physical validity of certain constitutive model in this context. Their remarks are based on the observation that the stresses of a second-order fluid are not integrable in the neighbourhood of a stick-slip singularity, Coates *et al.*[12] considered the flow behaviour of an UCM fluid near a re-entrant corner and they suggest that the stress are proportional to π^a where a is close to -1 and recently Davies and Devlin[13] reported similar stress proportionality, $\tau = \pi^{-0.985}$ as one of their inadmissible solutions of singular perturbation series with UCM-like asymptotic for a planar flow. We have seen that Weiessenberg number has pronounced effect on the vortex centre and this is documented in this communication. In this work, we encountered the corner singularity problem near the corner. This problem was examined in the paper of H. Demir *et al.*[14 & 15] and it was seen that viscoelastic fluid behaved differently from the Stokes flow and inelastic viscous flow.

The vorticity-stream function approach is one of the most popular methods for solving the 2-D flow equations. Although this method produces a well-behaved and tightly coupled equation set, it is restricted to two dimensional flow, since in three-dimensional flows the stream function does not exist. In this study, a change of variables has been made which replaces the velocity components with a vorticity (ω) and a stream function (Ψ).

MATHEMATICAL PROBLEM AND METHOD OF SOLUTION

Governing Equations

In this analysis, the flow is considered to be incompressible with constant properties. With regard to these assumptions, the continuity equation and the momentum equation can be expressed in dimensional form as follows :

$$\frac{\partial u}{\partial x}+\frac{\partial v}{\partial y}=0 \qquad \text{... (1)}$$

$$\left\{\begin{array}{l} \rho\left(u\frac{\partial u}{\partial x}+v\frac{\partial u}{\partial y}\right)=-\frac{\partial P}{\partial x}+\frac{\partial \sigma_{11}}{\partial x}+\frac{\partial \sigma_{12}}{\partial y} \\ \rho\left(u\frac{\partial v}{\partial x}+v\frac{\partial v}{\partial y}\right)=-\frac{\partial P}{\partial y}+\frac{\partial \sigma_{12}}{\partial x}+\frac{\partial \sigma_{22}}{\partial y}-\rho g \end{array}\right\} \qquad \text{... (2)}$$

The above equations representing the conversation of mass and momentum can be rewritten in terms of vorticity-stream function formulation (ω, Ψ). The vorticity is expressed as

$$\omega=\frac{\partial v}{\partial x}-\frac{\partial u}{\partial y} \qquad \text{... (3)}$$

The stream function Ψ is expressed in such a way that the continuity equation is identically satisfied. Then, we have

$$u=-\frac{\partial \Psi}{\partial y} \text{ and } v=\frac{\partial \Psi}{\partial x}. \qquad \text{... (4)}$$

Instead of solving (2) in terms of the primitive variables, the equations are rewritten in terms of the stream function and vorticity defined in eqs. (3) and (4).

$$\nabla^2 \Psi=\omega \qquad \text{... (5)}$$

and

$$\rho\left(u\frac{\partial \omega}{\partial x}+v\frac{\partial \omega}{\partial y}\right)=\frac{\partial^2}{\partial x\,\partial y}(\sigma_{22}-\sigma_{11})+\left(\frac{\partial^2}{\partial x^2}-\frac{\partial^2}{\partial y^2}\right)\sigma_{12}. \qquad \text{... (6)}$$

Eqs. (5) and (6) are known as the Poisson's equation and the vorticity transport equation, respectively. In order to provide continuity between the various studies in this area and also to guard against undesirable numerical overflows, it is often helpful to perform numerical investigations using non-dimensional variables. In this study, physical quantities are made dimensionless by using representative quantities. The non dimensionalized forms of eqs. (5) and (6) are as follows.

$$\nabla^2 \Psi=\omega \qquad \text{... (7)}$$

and

$$\left(u\frac{\partial \omega}{\partial x}+v\frac{\partial \omega}{\partial y}\right)=\frac{1}{\eta\, Re}\left[\frac{\partial}{\partial x}\left(\eta^2\frac{\partial \omega}{\partial x}\right)+\frac{\partial}{\partial y}\left(\eta^2\frac{\partial \omega}{\partial y}\right)\right]+\frac{F}{Re}, \qquad \text{... (8)}$$

where

$$F=M(\Psi)\,M(\eta)+L(\Psi)\,L(\eta)-\frac{M}{2}(S_{11}-S_{22})-L(S_{12})$$

and the operators are defined as $M(\cdot) = 2\dfrac{\partial^2(\cdot)}{\partial x\,\partial y}$; and $L(\cdot) = \dfrac{\partial^2(\cdot)}{\partial y^2} - \dfrac{\partial^2(\cdot)}{\partial x^2}$.

On taking the non-dimensionalised form of the governing equations we have two non-dimensional parameters namely 'Reynolds' number which is defined as $Re = \rho U l/\eta(0)$ and Weissenberg number which can be defined as the product of the relaxation time to the rate of shear of the fluid flow.

Solution Procedure

In order to sole the set of partial differential equations above, the finite-difference method was applied. An iterative procedure was adopted in the calculation. The convective terms and the second order partial derivates are discretised by central differencing. Uniform grid spacing was employed in both directions. The criteria used to check for the convergence criterion is

$$\underset{i,j}{Max}\left(\frac{\left|\phi_{i,j}^{n+1}-\phi_{i,j}^{n}\right|}{1+\left|\phi_{i,j}^{n}\right|}\right), \varepsilon,$$

where ϕ stands for Ψ and ω, separately. In the above criteria, n refers to iteration number, and i and j to space. The value of ε is prescribed to be 10^{-4} for vorticity and 10^{-5} for stream function.

Boundary Conditions

The corresponding boundary conditions for the problem are shown in Fig. 1.

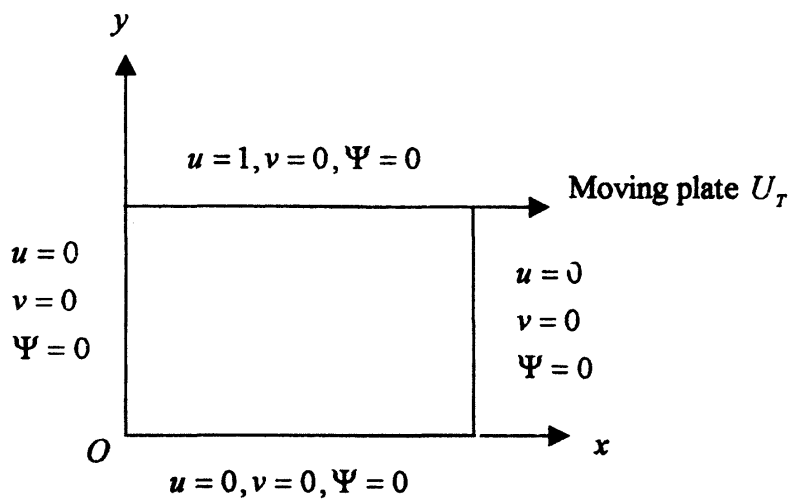

FIG. 1. Boundary conditions

The vorticity on the boundaries can be formulated in two ways. The first way is the Woods formula, based on interior values of stream-function and two levels of vorticity. An alternative to the Woods method is to use known stream function values only. We choose the known interior stream function values to solve the stream and vorticity equation for driven cavity flow.

In this work, the extra-stress is related to the deformation suffered by the fluid for general shear-rate (or deformation rate) ($\dot{\gamma}$) through a decomposition into a viscous solvent part $\overline{\sigma_{i,j}}$ is defined as the usual way with 'the stress directly proportional to rate of strain', i.e.

$$\overline{\sigma_{i,j}} = 2\,\eta(\dot{\gamma})\,d_{ij} \qquad \ldots (9)$$

where $\eta(\dot{\gamma})$ is a solvent viscosity and d_{ij} is the rate of strain. The polymeric part S_{ij} is modelled by the upper convected CEF model which is written as

$$S_{ij} = 4\,\chi(\dot{\gamma})\,d_{ik}\,d_{kj} - 2\,\zeta(\dot{\gamma})\,\overset{\nabla}{d}ij \qquad \ldots (10)$$

Therefore, we can write

$$\sigma_{ij} = \overline{\sigma_{i,j}} + S_{ij}$$

and

$$\sigma_{ij} = 2\,\eta(\dot{\gamma})\,d_{ij} + 4\,\chi(\dot{\gamma})\,d_{ik}\,d_{kj} - 2\,\zeta(\dot{\gamma})\,\overset{\nabla}{d}_{ij}. \qquad \ldots (11)$$

Here, $\chi(\dot{\gamma})$ and $\zeta(\dot{\gamma})$ generally are defined as

$$\chi(\dot{\gamma}) = \frac{1}{2}N_1(\dot{\gamma}) + N_2(\dot{\gamma}),\ 2\,\zeta(\dot{\gamma}) = N_1(\dot{\gamma}), \qquad \ldots (12)$$

where $N_1(\dot{\gamma})$ and $N_2(\dot{\gamma})$ are material functions known as the primary and secondary normal stress coefficients, respectively. However, in this work, we take the following forms of this

$$(i)\ N_1 = 2\,\lambda_1 \frac{(\eta(0) - \eta(\infty))}{1 + (\lambda\,\dot{\gamma})^{1-n}}\ (ii)\ N_2 = 0 \qquad \ldots (13)$$

and upper convected derivatives in eq. (2.6) is defined as

$$\overset{\nabla}{d}_{ij} = \frac{D}{Dt}d_{ij} - Zd_{ij} - d_{ij}Z^T, \qquad \ldots (14)$$

where

$$Z = \nabla \cdot V \text{ and } Z^T = (\nabla \cdot V)^T. \qquad \ldots (15)$$

Finally, the Cross model is used in this work for modelling of the viscosity function and this is known as

$$\eta(\dot{\gamma}) = \eta(\infty) + \frac{(\eta(0) - \eta(\infty))}{1 + (\lambda\,\dot{\gamma})^{1-n}}. \qquad \ldots (16)$$

RESULTS

We have presented all the results for flow patterns arising from the pseudoplastic flow configuration of the 2D model. Cavity driven flow, in the steady case, is solved by considering walls which are allowed to move with the top wall or both wall moving in the same direction, or with walls moving in the opposite directions for various aspect ratios.

In the 2D numerical simulation of viscous and viscoelastic fluids, We first considered the convergence properties of the numerical solutions for stream function and vorticity by comparing calculations for various grid widths for the Newtonian and non-Newtonian fluids near the top wall,

and comparing values of vorticity and stream function it is evident that convergence to 4 decimal places has been achieved for $Re = 1$ and $Re = 100$, as grid widths decreases. To show this for stream function near the top wall, we evaluated results and showed in Fig. 2.

A second comparison was made for a graphical comparison of the centre line u-velocity for a Reynolds number of 100 and 1000 obtained in this research with the ones available in the literature. In this case we examined the centre line u-velocity for viscous and viscoelastic fluids. In the literature only Newtonian and viscous non-Newtonian fluid data were readily found to compare with our results. Therefore, we compare our results qualitatively and quantitatively to establish the accuracy of the results obtained with those obtained by Tosaka[16] and Demir[17] and our results have been seen to be totally in agreement with the above researchers for viscous cases. These are shown in Figs. 5 and 6 and produced by Tosaka[16] and Demir[17] respectively. Our results are agree very well with those both qualitatively and quantitatively as seen Fig. 3. In addition, we present Criminale-Erickson-Filbey (CEF) fluid behaviour at $Re = 100$ and $Re = 1000$ as shown in Fig. 4 and this has been documented first. In addition to this, it can be said that viscous case shows similar behaviour to viscoelastic case for the same Reynolds number.

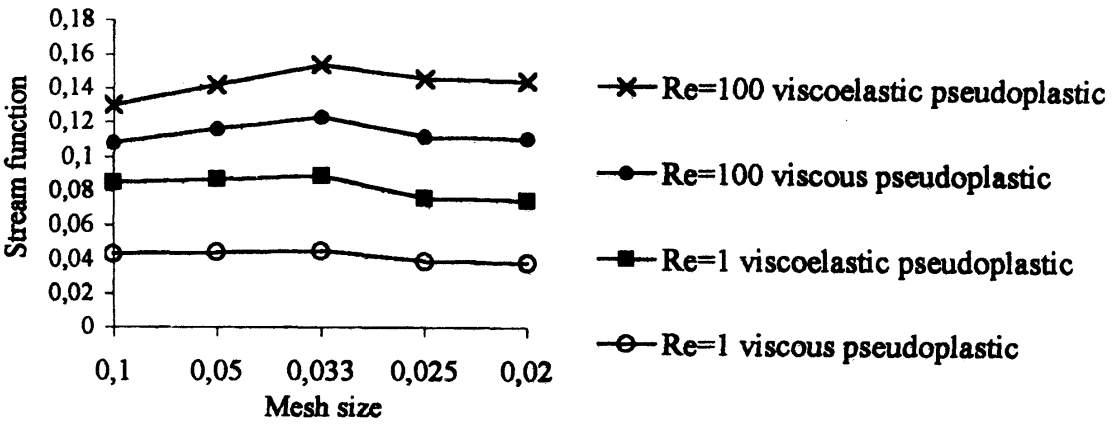

FIG. 2. Convergence criterion for stream function at $Re = 1$ and $Re = 100$

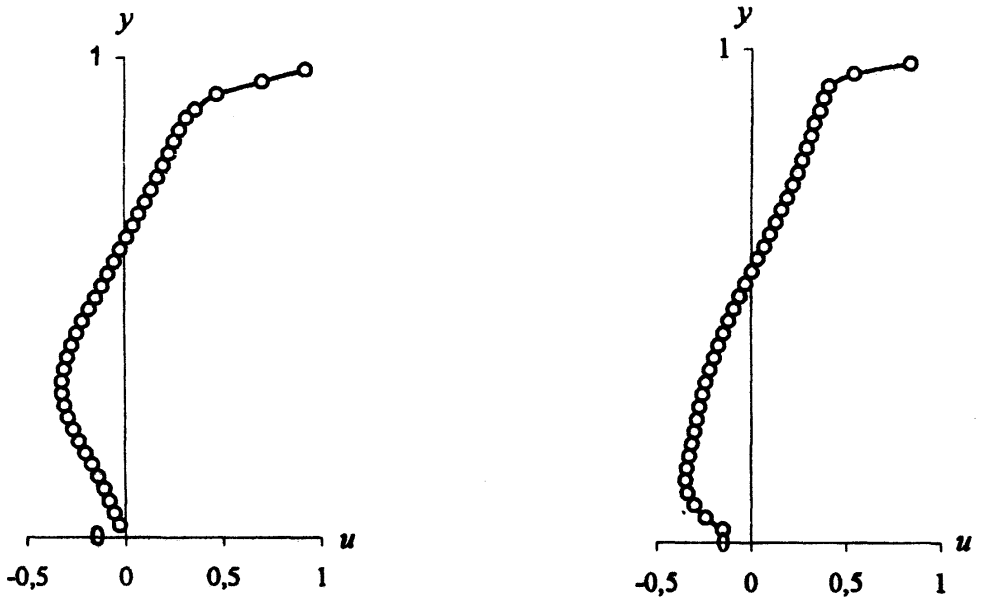

FIG. 3. u-velocity profile along vertical centre line at $Re = 1$ and $Re = 100$ $Re = 1000$ for pseudoplastic fluid respectively by Demir and Erturk

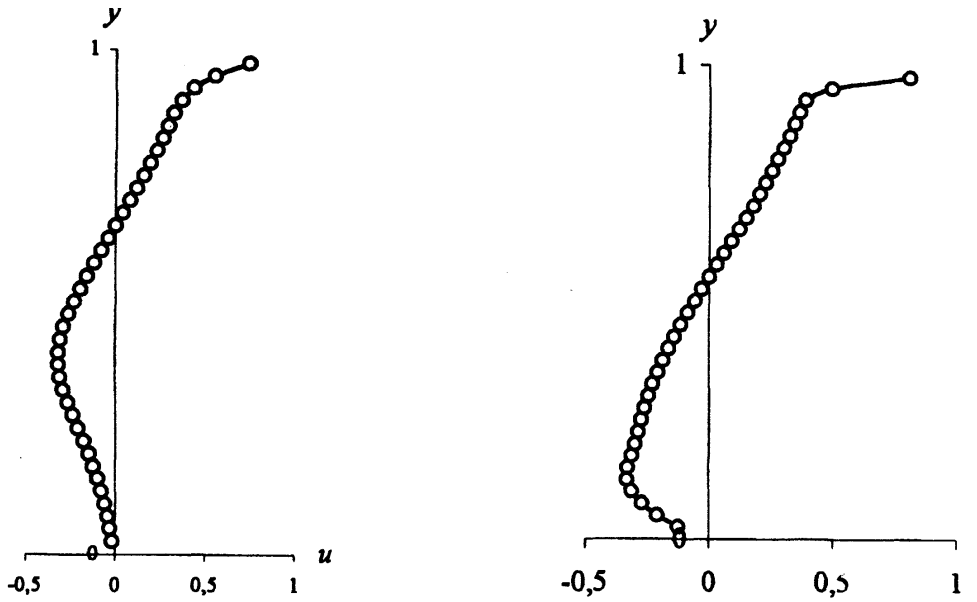

FIG. 4. u-velocity profile along vertical centre line at Re = 100 Re = 1000 for CEF pseudoplastic fluid respectively by Demir and Erturk

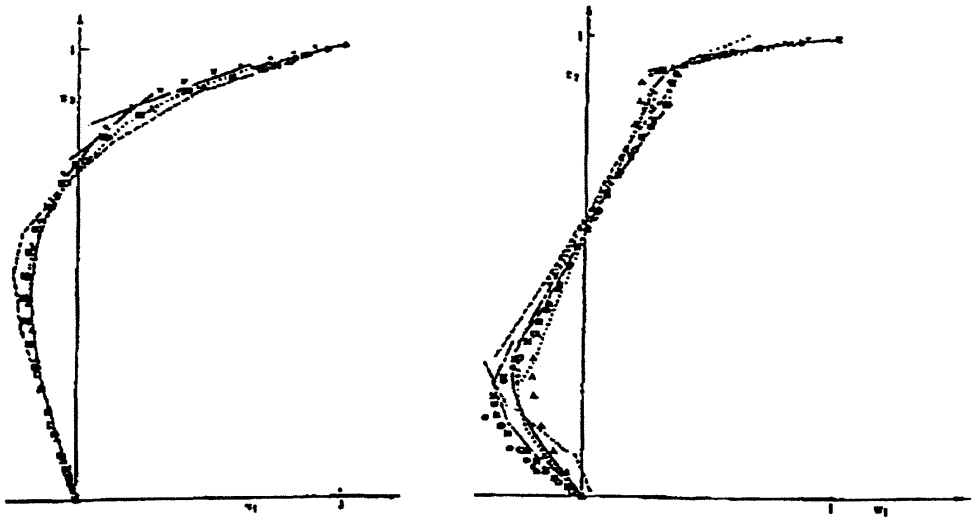

Comparison of u-velocity profiles along vertical centre line at Re = 100. Tosaka *et al* (o 23 by 25, Δ 21 by 21, ■ 25 by 25 BEM); □ Ghia *et al.* (129 by 129 FDM); XXX Burggraf (40 by 40 FDM); --- Thomasset FEM; ... Bercovier *et al.* FEM: - - Borrel FEM

Comparison of u-velocity profiles along vertical centre line at Re = 1000. Tosaka *et al* (o 23 by 25, Δ 21 by 21, ■ 25 by 25 BEM); □ Ghia *et al.* (129 by 129 FDM); ——Nallasamy *et al.* FDM; ... Bercovier *et al.* FEM: - - Benazeth FEM; - - Thomasset; +++ Figueroa FEM

FIG. 5. u-velocity profile along vertical centre line at Re = 100 Re = 1000 fby Tosaka *et al.*

We organise all results in terms of the following cases :

i) Standard cavity driven flow with the top wall moving.

ii) Two walls moving in the opposite direction.

iii) Two walls moving in the same direction.

iv) The Aspect Ratio of the cavity.

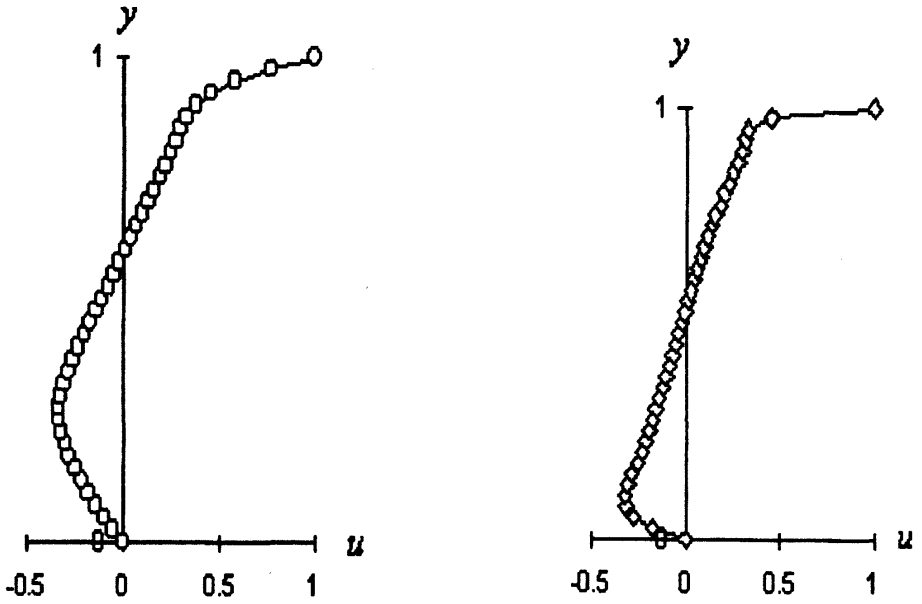

FIG. 6. u-velocity profile along vertical centre line at Re = 100 and Re = 1000 for pseudoplastic fluid respectively by Demir[17]

In this paper, the cavity flow problem was extended to viscoelastic fluids to seek the qualitatively different dynamical behaviour arising from the tendency of elasticity to opposite inertia. We obtained different flow patterns attributed to elasticity to opposite inertia at various types of the driven cavity flows of the geometry. Elastic and inelastic fluid flow show similar behaviour in the case top wall or both wall moving in the same direction with unit aspect ratio. These pictures will not been presented.

For the walls moving in the opposite direction the solution produced one main vortex and the streamlines almost take a "square" shape near the walls of the cavity. In the central part of the cavity the streamlines become more different from those of near the walls at Re = 1 shown in Fig. 7 for inelastic fluid. When elasticity was incorporated, there are two vortices which are symmetric

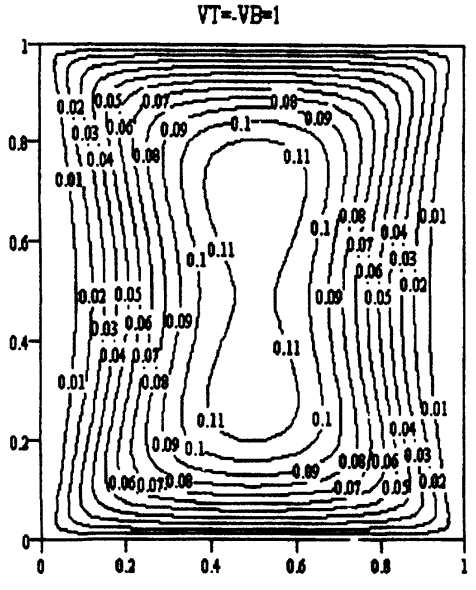

FIG. 7. Streamlines for viscous pseudoplastic flow at Re = 1

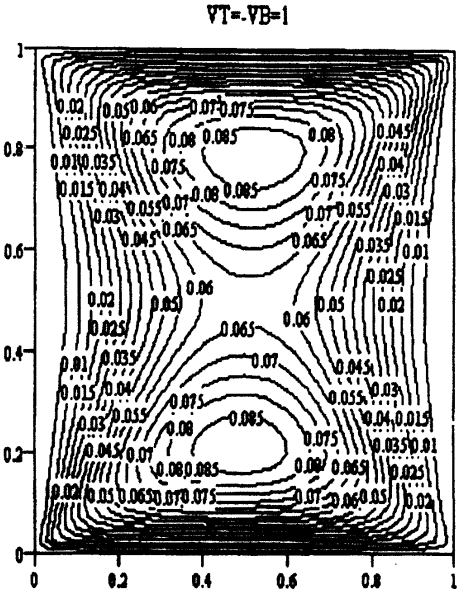

FIG. 8. Streamlines for viscous pseudoplastic flow at Re = 1

and located near the top and bottom half of the cavity, and are surrounded by an outer vortex and it can be seen in Fig. 8. In this case, the Weissenberg number are taken as $Wi = 0.1$.

Especially, comparison of Fig. 7 with Fig. 8 is very important, because this comparison shows clearly the effect of elasticity may be helpful for the experiment work. In this paper the effect of the aspect ratio for cavity driven flow is considered as well and flow patterns produced for two walls moving in the same or opposite directions for aspect ratio is 0.5. In this case viscous and viscoelastic case show similar behaviour as well.

We presented results only for aspect ratio is 2. For the two walls moving in the same direction we see that two counter-rotating vortices ar Re = 500. These vortex centres are located from top and bottom walls respectively at (0.53, 1.55) and (0.53, 0.44), shown in Fig. 9. When elasticity is involved two main vortices are produced in the configuration and they appear symmetric. The vortex centres were found to be (0.54, 1.58) and (0.54, 0.45) from the top and bottom walls shown in Fig. 10 respectively.

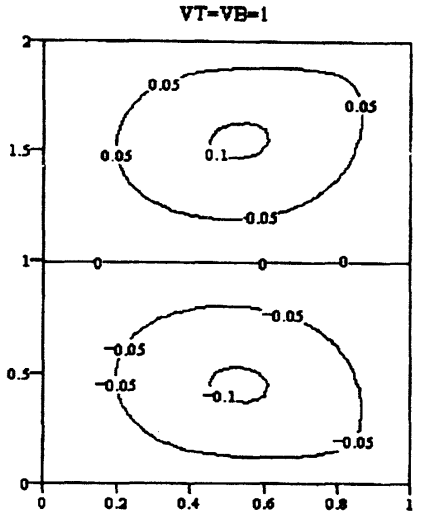

FIG. 9. Streamlines for viscous pseudoplastic flow at Re = 500

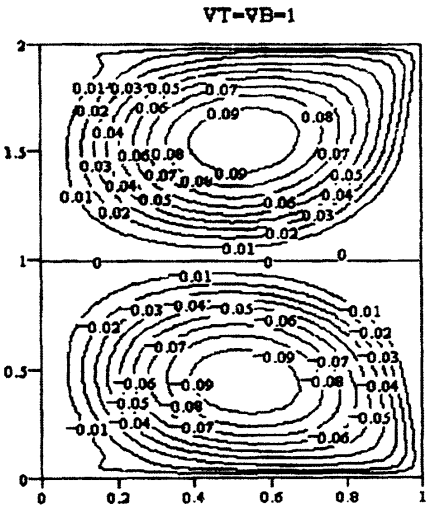

FIG. 10. Streamlines for viscous pseudoplastic flow at Re = 500

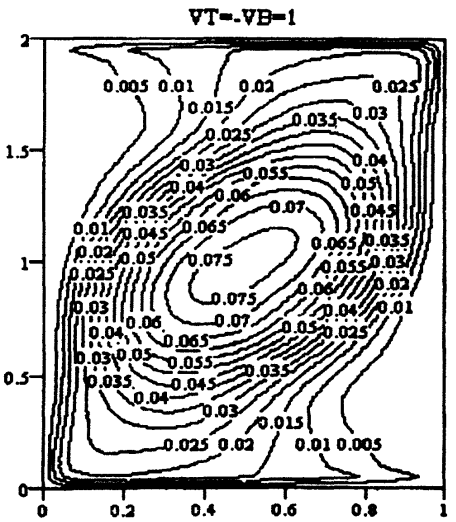

FIG. 11. Streamlines for viscous pseudoplastic flow at Re = 1000

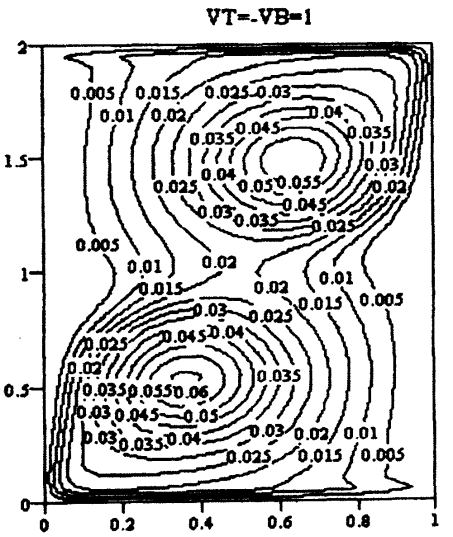

FIG. 12. Streamlines for viscous pseudoplastic flow at Re = 1000

For the two walls moving in the opposite direction one main vortex is found as shown in Fig. 11 at Re = 1000. When elasticity was incorporated we observed two vortices which are symmetric and located near the top and bottom half of the cavity and surrounded by an outer vortex as shown in Fig. 12.

CONCLUSION

This paper mainly consists of the computer simulation and analysis of the streamline structures of inelastic and CEF pseudoplastic fluids in 2D cavity. It is seen that the solutions for wall driven cavity flow are stable and convergent for some of Reynolds number and power index in case of inelastic viscous flow. But for CEF fluid the instability occurs and it is seen that these solutions are unstable and divergent in case of high Weissenberg number even for small Reynolds number. Therefore, we seek the critical Weissenberg number and is found as Wi = 0.1. Since instabilities are characterised by this control parameters: the Reynolds and Weissenberg numbers, the effect of inertia and elasticity are of particular interest as well as the aspect ratios. To show this several cases investigated for different wall driven and aspect ratios of cavity low. We found different flow behaviour with respect to the streamline structures at Re = 1 in case of two walls moving in the opposite direction, for unit aspect ratio. When aspect ratios are undertaken, we have seen that different flow behaviour as well. In this case for aspect ratio is 2, viscous and viscoelastic fluids are generated different streamlines structures at Re = 500 and 1000 respectively. These behaviours have been seen that as an elasticity effect of the fluid. Moreover, we believe that more work need to be done in this subject. Therefore, we will try to solve this problem by using Pseudo-Spectral Finite Difference method. To this, special functions which satisfy the boundary condition in one spectral variables are used and Galerkin Equations are evaluated at the Chebyshev grid.

REFERENCES

1. J. D. Bozemann and C. Dalton. *J. comput. Phys.* **12** (1973) 348-63.
2. F. H. Ling and X. Zhang, *J. Fluids Engng.*, **117** (1995) 75-80.
3. O. B. Burggraf, *J. Fluid Mech.*, **24** (1966) 113-51.
4. M. Kawaguti, *Numerical Solution of the Navier-Stokes Equations for the Flow in a Two Dimensional Cavity J. phys. Soc. Japan.* **16** (1961) 2307.
5. F. Pan and A. Acrivos, *J. Fluid Mech.*, **28** 643-55.
6. G. K. Batchelor, *J. Fluid Mech.* (1956) 177-90.
7. D. D. Joseph, M. Renardy and J. C. Saut, *Arch. ratn. Mech. Anal.* **87** (1987) 213.
8. R. A. Brown, A. N. Armstrong, A. N. Beris and P. W. Yeh, *Comput. Methods Appl. Mech. Engng.* (1986) 201.
9. A. N. Beris, R. C. Armstrong and R. A. Brown, *J. non-Newtonian Fluid Mech.* **22** (1987) 129-67.
10. S. A. Orszag and L. C. Kells, *J. Fluid Mech.* **96** (1980) 159.
11. G. G. Limpcomb, M. M. Den, Du Hur and D. V. Boger, **26** (1988) 297-325.
12. P. J. Coates, R. C. Armstrong and R. A. Brown, *J. non-Newtonian Fluid Mech.* **42** (1992) 141-88.
13. A. R. Davies and Devlin, *J. non-Newtonian Fluid Mech.* **50** (1993) 173-91.
14. H. Demir and F. T. Akyildiz, (1999) *"Unsteady Thermal Convection of a Non-Newtonian Fluid", Paper accepted as a publication in Int. J. Engng. Sci.*
15. H. Demir, R. W. Williams and F. T. Akyildiz, *The singularities Near the Corner of a Viscoelastic Fluid in a 2D Cavity. Math. comput. Appl.* **4** (1999) 39-44.
16. N. Tosaka, Development of BEM for Convective Viscous Flow Problems, *Int. J. Solid Struct.* **31** (1994) 1847-59.
17. H. Demir, The Stability Properties of Some Rheological Flows. *PhD Thesis* Dept. of Math and Computing, The University of Glamorgan.
18. J. M. Ottino and R. Chella, *Polymer Engng Sci.* **23** (1983) 364-79.
19. G. P. Sasmal, *J. non-Newtonian Fluid Mech.* **56** (1995) 15-47.
20. J. R. Douglas and D. W. Peacement, *AICHE J.* **1** (1955) 502-12.